CHEMISTRY OF MATERIALS | 25th Anniversary

Article

Synthesis of novel orthorhombic Mo and V based complex oxides coordinating alkylammonium cation in its heptagonal channel and their application as a catalyst

Satoshi Ishikawa, Toru Murayama, Shunpei Omura, Masahiro Sadakane, and Wataru Ueda

Chem. Mater., **Just Accepted Manuscript** • DOI: 10.1021/cm400239c • Publication Date (Web): 02 May 2013

Synthesis of novel orthorhombic Mo and V based complex oxides coordinating alkylammonium cation in its heptagonal channel and their application as a catalyst

Satoshi Ishikawa[a)], Toru Murayama [a)]*, Shunpei Ohmura [a)], Masahiro Sadakane [b)], Wataru Ueda [a)]*

[a)] Catalysis Research Center, Hokkaido University, N-21, W-10, Sapporo, 001-0021, Japan

[b)] Department of Applied Chemistry, Graduate School of Engineering, Hiroshima University, 1-4-1 Kagamiyama, Higashi-Hiroshima, 739-8527, Japan

E-mail: ueda@cat.hokudai.ac.jp, murayama@cat.hokudai.ac.jp.

Mo-V-O complex oxide, alkylammonium isopolymolybdate, orthorhombic structure, selective oxidation of ethane.

ABSTRACT: The effects of several alkylammonium cations on the synthesis of orthorhombic $Mo_3VO_{11.2}$ complex oxides (MoVO) were investigated. First, we synthesized various alkylammonium isopolymolybdates as precursors for the synthesis of MoVO. Methylammonium heptamolybdate, dimethylammonium trimolybdate, ethylammonium trimolybdate and ethylenediammonium trimolybdate were obtained as pure materials in new crystalline structures. Orthorhombic MoVO complex oxides were synthesized under hydrothermal conditions when $(CH_3NH_3)_6Mo_7O_{24}$ and $((CH_3)_2NH_2)_2Mo_3O_{10}{\cdot}H_2O$ were used. It was found for the first case that methylammonium cations and dimethylammonium cations were incorporated into the orthorhombic MoVO structure, forming compounds of $Mo_{32.3}V_{7.7}O_{112}(CH_3NH_3)_{4.0}{\cdot}9.7H_2O$ and $Mo_{30.2}V_{9.8}O_{112}((CH_3)_2NH_2)_{2.5}{\cdot}8.5H_2O$, respectively. These alkylammonium cations play an important role as a stabilizer in the synthesis of MoVO and act like as a structure-directing agent for the orthorhombic phase.

KEYWORDS: Mo-V-O complex oxide, alkylammonium isopolymolybdate, orthorhombic structure, selective oxidation of ethane.

INTRODUCTION

Mo–V–M–O (M= Nb, Te, Sb, etc.) complex oxide catalysts have attracted interest in the selective oxidation and the ammoxidation of light alkanes [1-16]. We have recently reported a hydrothermal synthesis method for preparing single phase Mo and V based complex metal oxides (MoVO) with orthorhombic structure and successfully demonstrated the roles of the elements of the catalysts in the catalysis [17-20]. The orthorhombic MoVO is a layered structure with slabs with 4.0 Å *d*-spacing and the slabs stack each other with anisotropically growing along the *c*–axis to form a rod crystal. The *a*-*b* plane of the orthorhombic MoVO is composed by the arrangement of the pentagonal $\{Mo_6O_{21}\}$ units and MO_6 (M = Mo, V) octahedra with the formation of hexagonal and heptagonal ring channels [21-25].

We proposed that the pentagonal $\{Mo_6O_{21}\}$ unit derived from ammonium heptamolybdate (AHM) is a building block in the synthesis of the orthorhombic MoVO under hydrothermal conditions [26-31]. Ammonium ion, as a counter cation of the Mo precursor, is confined in the heptagonal channel of MoVO during the crystal growth (Fig. 1). This ammonium cation can be removed by heat treatment at 673K in air or under N_2 flow without collapse of the crystalline structure and with formation of Brønsted acid sites which may relate to the catalytic activity of MoVO. The ammonium cation is not only for charge compensation but also regarded as a structure-directing agent like in the synthesis of aluminosilicates. This suggests that alkylammonium cations with different molecular size have effects on the crystallization of MoVO and on crystalline state as structure-directing agents.

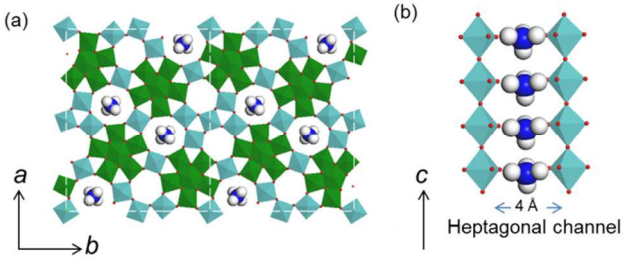

Fig. 1 Structure model of orthorhombic MoVO complex oxide and ammonium cation: *a*-*b* plane (a) and image of heptagonal channel (b). (green: pentagonal $\{Mo_6O_{21}\}$ unit, light blue: Mo or V octahedral, red: oxygen, blue: nitrogen and white: hydrogen)

Organic structure-directing agents with appropriate size and shape should be selected for efficient crystallization [32-34]. A variety of organic structure-directing agents have been studied in zeolites [35], mesoporous oxides of the MCM-41 class [36-37], biomineralized materials [38], and microporous octahedral–tetrahedral or square pyramidal–tetrahedral transition metal phosphate frameworks (TMPO) [39-40]. Although in the case of the orthorhombic MoVO catalyst the structural space in the heptagonal channel is 4.0 Å diameter and limits to counter cations with smaller molecular size like an ammonium cation with 2.8 Å size, organic structure-directing agents may afford advantages in the self-assembly process of the building units to form the crystalline structure.

The synthesis of alkylammonium isoplolymolybdate has also attracted extensive interest as hybrid organic-inorganic materials for electron conductivity, magnetism and photochemistry. There are reports about the synthesis of crystalline alkylammonium isopolymolybdate [41-45]. A large number of alkylammonium isopolymolybdates have been isolated using secondary and tertiary amines, whereas only a few alkylammonium isopolymolybdates of (di-, tri-) methylamine, ethylamine, propylamine, ethylenediamine and propyldiamine have been investigated [references].

In this paper, several alkylammonium isopolymolybdates were prepared with the above amines and characterized. Then, crystalline orthorhombic MoVO were hydrothermally synthesized by using the prepared alkylammonium isopolymolybdates instead of AHM. We found that the obtained MoVO possessed the alkylammonium cations in the heptagonal channel of the structure. This is the first example of orthorhombic MoVO crystal containing the alkylammonium cation in the structure.

EXPERIMENTAL SECTION

Preparation of alkylammonium isopolymolybdate by evaporation. The preparation method for methylammonium ispolymolybdate are shown as a typical example. 22.594 g of MoO_3 (0.150 mol, Kanto) was dissolved in 33.2 ml of 40% methylamine solution (methylamine: 0.300 mol, Wako). After completely dissolved, the solution was evaporated under vacuumed condition of P/P_o= 0.03 at 343 K and then solid powder was obtained. The powder was dried in air at 353 K overnight. Thus prepared alkylammonium isopolymolybdate is abbreviated as MAHM (methylammonium heptamolybdate). The details preparation method and abbreviated name for other alkylammonium isopolymolybdates were described in supporting information.

Preparation of alkylammonium isopolymolybdate by precipitation. In the case of ethylenediamine, 1,2–propanediamine and 1,3–propanediamine, 40 ml of 35% of HCl (HCl: 1.3 mol, Wako) was added into the mixture solution of amine solutions (0.30 mol) and 22.594 g of MoO_3 (0.15 mol), then stirred for 30 min. During stirring, white crystal powder was deposited. Then, the powder was washed with 1 L of water and dried in air at 353 K overnight. These prepared powder were abbreviated as EDATM (ethylenediammonium trimolybdate), 1,2–PDATM (1,2–propanediammonium trimolybdate), and 1,3–PDATM(1,3–propanediammonium trimolybdate).

Preparation of MoVO mixed oxide. $(NH_4)_6Mo_7O_{24}\cdot 4H_2O$ (Mo: 50 mmol, Wako) or prepared alkylammonium isopolymolybdate (Mo: 50 mmol) was dissolved in 120 mL of distilled water. Separately, an aqueous solution of $VOSO_4$ (Mitsuwa Chemicals) was prepared by dissolving 12.5 mmol of hydrated $VOSO_4$ in 120 mL distilled water. These two solutions were mixed at 293 K and stirred for 10 min before being introduced into an autoclave (300 mL Teflon inner tube). After 10 min of nitrogen bubbling to replace the residual air, hydrothermal reaction was carried out at 448 K for 48 hours. Obtained gray solids were washed with distilled water and dried at 353 K overnight. These solids were purified by treatment with oxalic acid; dry solids were added to an aqueous solution of oxalic acid (0.4 M; 25 mL / 1 g solids) and this mixture was stirred at 333 K for 30 min. Solids were isolated from the suspension by filtration, washed with distilled water, and dried at 353 K overnight. Yield of the catalyst was calculated based on MoO_3 and V_2O_5.

Characterizations of catalyst. Powder XRD patterns were recorded on a diffractometer (RINT Ultima+, Rigaku) with Cu-Kα radiation. For XRD measurement, samples were ground and put on a horizontal sample holder. Diffraction patterns were recorded in 2 theta = 4 – 60°. Raman spectra (inVia Reflex Raman spectrometer, RENISHAW) were taken in air on a static sample with Ar laser powers. Each spectrum was collected for 10 s accumulated once and normalized for comparison. CHN elemental composition was determined using Micro Corder JM10 (Yanaco). TG analysis was carried out in an air flow (50 ml min^{-1}) by using TG8120 (Rigaku). The sample (ca. 0.01 g) was placed on a sample pan and the temperature was raised at a rate of 10 K min^{-1}. FT-IR analysis was carried out using a spectrometer (FT/IR-660, JASCO) with a MCT detector. IR spectra were obtained by integration of more than 256 scans with a resolution of 4 cm^{-1}. X-ray photoelectron spectroscopy (XPS) measurements were carried out using JPS-9010MC spectrometer (JEOL) with Al irradiation and monochromator. ICP–AES was carried out with a VISTA–PRO apparatus (Varian). N_2 adsorption was performed at 77 K in a gas adsorption analyzer (BELSORP-max; BELJAPAN, Inc. Japan). The measurements were performed at relative pressures from 10^{-8} to 1.0 in an incremental dose mode. Prior to the adsorption measurements, samples were outgassed at 573 K under vacuum for 2h. Pore volume and external surface area were calculated by *t*-plot method in the *t*-range from 0.15 to 0.90. TPD was carried out using a BELSORP apparatus. The measurement procedure is as follows: 50 mg of samples were set between two layers of quartz wool and left under 50 mL min^{-1} He at 313 K for 40 min. Then, desorption profile was recorded with a mass spectrometer (M-200GA-DM, Anelva Co.) from 313 K to 873 K with the ramp rate at 10 K min^{-1} under helium flow. The following

desorption species were monitored by corresponding *m/z* species: H_2O (*m/z*= 18), NH_3 (*m/z*= 16), N_2 (*m/z*= 14, 28), CO (*m/z*= 12, 28), CO_2 (*m/z*= 44), CH_3NH_2 (*m/z*= 31), and $C_2H_5NH_2$ (*m/z*= 45).

Catalytic test for ethane selective oxidation. Ethane selective oxidation tests were performed at atmospheric pressure using a fixed-bed flow reactor. The inner diameter of the catalyst bed was 10 mm and the length was 30 mm. The catalysts ground in an agate mortar were calcined in air at 673K for 2 h beforehand. The obtained samples were diluted with SiO_2 (50-80 mesh, Miyazaki Chemicals). Then, the mixed powder (net catalyst weight; 0.5 g) was set into the reactor and heated at 623K under N_2 flow (40 mL min^{-1}). N_2 gas was replaced to the reaction gas with the composition of $C_2H_6/O_2/N_2$= 1: 1: 8 (the total flow rate was 50 mL min^{-1}) and the condition was kept for 2 h at 623K. Then the catalytic test was started at the reaction temperature of 573 K. The reactants and products were analyzed with three on-line gas chromatographs, Molecular Sieve MS13X with TCD (for O_2, N_2 and CO), Gaskuropack 54 with TCD (for CO_2, C_2H_4 and C_2H_6), and Porapak Q with FID (for CH_3COOH). The carbon balance was always more than 98%.

RESULTS AND DISCUSSION

Characterization of prepared alkylammonium isopolymolybdates. Alkylammonium isopolymolybdates were prepared and isolated. MAHM, DMATM, TMATM, EATM and PAHM were synthesized by the evaporation, while EDATM, 1,2–PDATM and 1,3–PDATM were synthesized by the precipitation method. Obtained isopolymolybdates were dried at 353K and analyzed by the Raman spectroscopy in order to identify the species of molybdate anion. Fig. 2 shows Raman spectra of AHM and the prepared alkylammonium isopolymolybdate. All samples exhibit a strong band around 930–950 cm^{-1}, which are characteristic stretching modes of Mo=O bonds [41]. AHM sample showed the Raman band at 937 cm^{-1} which can be attributed to the asymmetric stretching vibrations of Mo=O bond of heptamolybdate ($Mo_7O_{24}^{6-}$) anion. This band was also observed in MAHM and PAHM at 940 cm^{-1}, indicating the formation of $Mo_7O_{24}^{6-}$ in these compounds too. The other alkylammonium isopolymolybdates (DMATM, TMATM, EATM, EDATM, 1,2–PDATM and 1,3–PDATM) showed the band at 950 cm^{-1} which can be attributed to the asymmetric stretching vibrations of Mo=O bond of trimolybdate ($Mo_3O_{10}^{2-}$) anion. Observed other week bands beside the main bands might be ascribable to vibrations of Mo-O-Mo of the isopolymolybdates with band shifts depending on alkylammonium cations.

It is well known that pH value and cationic species affect the formation of molybdate anion [41]. MoO_4^{2-} anion is produced when MoO_3 is dissolved in alkaline solution. The dominant molybdate species in aqueous solution depending on pH are MoO_4^{2-} (pH>6.3), $Mo_7O_{24}^{6-}$ (pH=5.0) and $Mo_3O_{10}^{2-}$ (pH=4.0). In the present work, the predominant species were either $Mo_7O_{24}^{6-}$ or $Mo_3O_{10}^{2-}$ depending on alkylammonium cations. In the case of MA, PA, TMA, DMA, and EA, the initial pH values of the mixture solution of alkylamine (0.30 mol) and MoO_3 (0.15 mol) were 8.55, 6.93, 8.45, 7.91, and 7.55, respectively, so that the isopolymolybdate anions of either of $Mo_7O_{24}^{6-}$ or $Mo_3O_{10}^{2-}$ were formed by the simple evaporation method. On the other hand, in the synthesis of EDATM, 1,2–PDATM, and 1,3–PDATM, the initial pH values of the mixture solution were 8.93, 8.55, and 9.88, respectively. The pH values were so high that isopolymolybdates such as $Mo_7O_{24}^{6-}$ or $Mo_3O_{10}^{2-}$ were not formed by the evaporation but compounds of molybdate anion (MoO_4^-) was generated. These molybdates were identified as $(NH_2CH_2CH_2NH_2)MoO_3$, $(NH_2CH_2CH_2(NH_2)CH_2)MoO_3$ and $(NH_3CH_2CH_2CH_2NH_3)MoO_4$ by CHN analysis and Raman spectra [46]. We found that these alkylammonium molybdates afforded no MoVO materials. Therefore, we employed the precipitation method with the addition of HCl for these amines. The adjusted pH values of the solution were 6.12 (EDA), 4.65 (1,2–PDA) and 6.72 (1,3–PDA) and as expected, alkylammonium molybdates of $Mo_3O_{10}^{2-}$ were obtained.

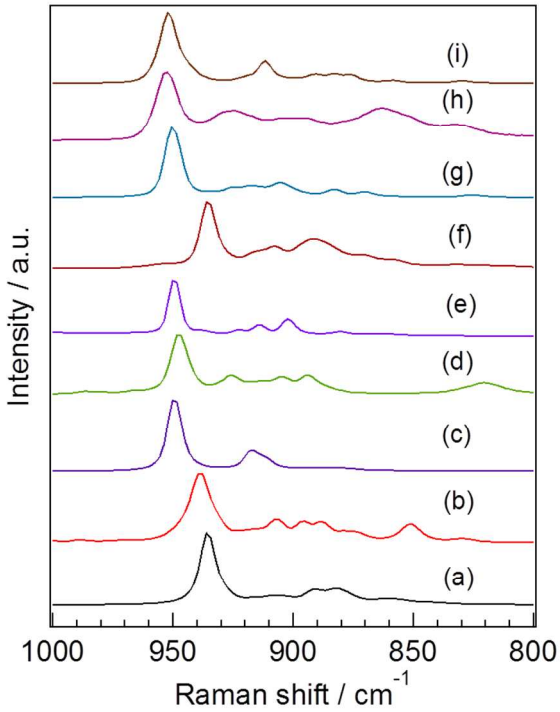

Fig. 2 Raman spectra of alkylammonium isopolymolybdates, (a) AHM; (b) MAHM; (c) DMATM; (d) TMATM; (e) EATM; (f) PAHM; (g) EDATM; (h) 1,2-PDATM; (i) 1,3-PDATM.

Table 1 shows the results of CHN elemental analysis and the percentage degree of weight loss measured by thermal gravimetric (TG) analysis. Chemical formula for each alkylammonium isopolymolybdate was determined on the basis of stoichiometry between isopolymolybdates anions and alkylammonium cations. Then the values of CHN were calculated. Theoretical weight loss was calculated from the chemical formulas and by assuming that the residue was MoO_3 after the analysis of TG. These calculated values are also summarized in Table 1. The ob-

tained data showed good agreements between the calculated elemental composition and the percent weight loss, suggesting that corresponding stoichiometric alkylammonium isopolymolybdates were formed and isolated. It should be noted that in the case of PAHM, the measured values were well-consistent with the calculated CHN and the percent weigh loss by assuming the composition of $CH_3CH_2CH_2NH_2$ $(CH_3CH_2CH_2NH_3)_6Mo_7O_{24}$ in which neutral $CH_3CH_2CH_2NH_2$ is occluded. Fig. S1 shows the XRD patterns of MoO_3 (starting material), AHM (reagent) and synthesized alkylammonium isopolymolybdates. MoO_3 gives the main peaks at 2θ= 12.6, 23.3, 25.6, 27.3 and no these diffractions were observed in the obtained alkylammonium isopolymolybdates. The XRD Patterns of the synthesized alkylammonium isopolymolybdates did not match those of related compounds in the database of the International Centre for Diffraction Data (ICDD). These are considered new patterns of single phasic crystal powders. Thus, the patterns of the x-ray powder diffraction were indexed and the symmetry and cell dimensions were calculated with the X-Cell (Powder Indexing, Accerlys). The calculated results were refined by Pawley method after indexing.

Fig. S2 shows the simulated patterns for MAHM, DMATM, EATM and EDATM. The crystal group of DMATM, EATM and EDATM were found to be orthorhombic (space group C2) and the crystal group of MAHM was found to be monoclinic (space group C121). Yamase et al. reported that DMATM was synthesized by the precipitation method from $Na_2MoO_4.2H_2O$ and $(CH_3)_2NCS_2{\cdot}2H_2O$ with the addition of hydrochloric acid [43]. EDATM synthesized by hydrothermal method was reported by Guillou et al. [44]. The XRD patterns of DMATM and EDATM prepared by the evaporation method employed here were different from those reported in the literatures. No structural reports were found concerning MAHM and EATM to the best of our knowledge. 1,3-PDATM Synthesized under hydrothermal conditions was reported by Ding et al. and possessed a triclinic structure [45]. However, 1,3-PDATM synthesized by the precipitation method in the present work gave a different diffraction pattern. Since it was difficult to obtain crystal information on TMATM, PAHM and 1, 2–PDATM due to their poor crystallinity, we are undertaking experiments to find suitable synthetic conditions.

The characterization data of obtained material were summarized below.

$(CH_3NH_3)_6Mo_7O_{24}$ (MAHM): Anal. Calcd for $(CH_3NH_3)_6Mo_7O_{24}$: C, 5.8; H, 2.9; N, 6.7. Found: C, 5.8; H, 2.8; N, 6.8. IR (1700-500 cm^{-1}): 1616, 1540, 1497, 1483, 1461, 1430, 1390, 1257, 1006, 973, 933, 914, 902, 885, 864, 834, 662, 634 cm^{-1}. Raman (1000-800 cm^{-1}): 937, 906, 895, 888, 851 cm^{-1}. TG-DTA: 423~473 K, -6.6% (endothermic); 473~533 K, -4.2%; 533~563 K, -6.1% (exothermic); 563~673 K, -3.8% (exothermic). The crystal phase of MAHM was monoclinic (space group C121) phase with a = 16.508, b = 11.254, c = 15.542 Å, $\alpha = \gamma = 90°$, β = 100.0°, Vc = 2887.4 $Å^3$. The structure model was refined to R_{wp} = 19.63% and R_p = 13.89% for 914 reflection peaks.

$((CH_3)_2NH_2)_2Mo_3O_{10}{\cdot}H_2O$ (DMATM) : Anal. Calcd for $((CH_3)_2NH_2)_2Mo_3O_{10}{\cdot}1H_2O$: C, 8.6; H, 3.2; N, 5.0. Found: C, 8.7; H, 3.1; N, 5.1. IR (1700-500 cm^{-1}): 1633, 1600, 1462, 1433, 1415, 1383, 1230, 1030, 1017, 936, 926, 911, 897, 884, 827, 789, 649, 611, 593, 579, 570, 557, 531, 521, 508 cm^{-1}. Raman (1000-800 cm^{-1}): 950, 916 cm^{-1}. TG-DTA: 423~473 K, -3.9% (endothermic); 473~563 K, -8.8% (exothermic); 563~763 K, -5.1% (small exothermic). The crystal phase of DMATM was orthorhombic (space group C2) phase with a = 20.772, b = 10.775, c = 7.973 Å, $\alpha = \beta = \gamma = 90°$, Vc = 1784.5 $Å^3$. The structure model was refined to R_{wp} = 7.66% and R_p = 17.92% for 824 reflection peaks.

$((CH_3)_3NH)_2Mo_3O_{10}$ (TMATM): Anal. Calcd for $((CH_3)_3NH)_2Mo_3O_{10}$: C, 12.7; H, 3.5; N, 4.9. Found: C, 12.7; H, 3.5; N, 5.0. IR (1700-500 cm^{-1}): 1620(s), 1480(s), 1454, 1416, 1370, 1046, 986(s), 928(s), 900(s), 840, 817, 712(s), 696(s) cm^{-1}. Raman (1000-800 cm^{-1}): 948, 925, 904, 893, 820cm^{-1}. TG-DTA: 373~423 K, -5.5% (endothermic); 423~523 K, -6.6% (endothermic); 523~583 K, -8.1% (exothermic); 583~733 K, -4.5% (exothermic).

Table. 1 Elemental composition of prepared alkylammonium isopolymolybdate analyzed by CHN elemental analysis and TGA

Abbreviation of alkylammonium isopolymolybdates	Composition of alkylammonium isopolymolybdates	C [wt%]		H [wt%])		N [wt%]		weight loss[wt%]	
		obs.	(calc.)	obs.	(calc.)	obs.	(calc.)	obs.	(calc.)
MAHM	$(CH_3NH_3)_6Mo_7O_{24}$	5.8	(5.8)	2.8	(2.9)	6.8	(6.7)	20.7	(19.2)
DMATM	$((CH_3)_2NH_2)_2Mo_3O_{10}\cdot 1H_2O$	8.7	(8.6)	3.1	(3.2)	5.1	(5.0)	17.8	(19.7)
TMATM	$((CH_3)_3NH)_2Mo_3O_{10}$	12.7	(12.7)	3.5	(3.5)	5.0	(4.9)	24.7	(24.0)
EATM	$(CH_3CH_2NH_3)_2Mo_3O_{10}$	9.0	(8.9)	2.9	(3.0)	5.2	(5.2)	18.7	(19.7)
PAHM	$CH_3CH_2CH_2NH_2$ $(CH_3CH_2CH_2NH_3)_6Mo_7O_{24}$	17.1	(17.1)	4.8	(4.7)	6.7	(6.6)	28.1	(31.7)
EDATM	$(NH_3CH_2CH_2NH_3)Mo_3O_{10}\cdot 1H_2O$	4.7	(4.6)	2.4	(2.3)	5.5	(5.3)	15.8	(15.3)
1,2-PDATM	$(NH_3CH_2CH(NH_3)CH_3)Mo_3O_{10}\cdot 1H_2O$	6.9	(6.6)	2.4	(2.6)	5.4	(5.2)	17.1	(17.6)
1,3-PDATM	$(NH_3CH_2CH_2CH_2NH_3)Mo_3O_{10}\cdot 1H_2O$	6.7	(6.6)	2.8	(2.6)	5.2	(5.2)	17.1	(17.6)

$(CH_3CH_2NH_3)_2Mo_3O_{10}$ (EATM): Anal. Calcd for $(CH_3CH_2NH_3)_2Mo_3O_{10}$: C, 8.9; H, 3.0; N, 5.2. Found: C, 9.0; H, 2.9; N, 5.2. IR (1700-500 cm^{-1}): 1613, 1510, 1482, 1458, 1403, 1319, 1201, 1051, 996, 983, 953, 928, 916, 890, 880, 864, 793, 786, 652, 605, 573, 562, 552, 543, 526, 503 cm^{-1}. Raman (1000-800 cm^{-1}): 950, 915, 902 cm^{-1}. TG-DTA: 473~543 K, -9.8% (exothermic); 563~663 K, -5.1%; 663~733 K, -3.8% (exothermic). The crystal phase of EATM was orthorhombic (space group C2) phase with a = 7.598, b = 22.424, c = 15.776 Å, $\alpha = \beta = \gamma = 90°$, Vc = 2687.90 $Å^3$. The structure model was refined to R_{wp} = 6.84% and R_p = 10.08% for 454 reflection peaks.

$CH_3CH_2CH_2NH_2$ $(CH_3CH_2NH_3)_6Mo_7O_{24}$ (PAHM): Anal. Calcd for $CH_3CH_2CH_2NH_2$ $(CH_3CH_2CH_2NH_3)_6Mo_7O_{24}$: C, 17.1; H, 4.7; N, 6.6. Found: C, 17.1; H, 4.8; N, 6.7. IR (1700-500 cm^{-1}): 1612(s), 1503, 1470, 1392, 1193, 1128, 902(s), 884(s), 863(s), 662(s), 636(s) cm^{-1}. Raman (1000-800 cm^{-1}): 935, 907, 891cm^{-1}. TG-DTA: 373~393 K, -13.1% (exothermic), 393~533 K, -8.0% (exothermic), 533~733 K, -7.0% (exothermic).

$(NH_3CH_2CH_2NH_3)Mo_3O_{10}\cdot H_2O$ (EDATM): Anal. Calcd for $(NH_3CH_2CH_2NH_3)Mo_3O_{10}\cdot 1H_2O$: C, 4.6; H, 2.3; N, 5.3. Found: C, 4.7; H, 2.4; N, 5.5. IR (1700-500 cm^{-1}): 1630, 1616, 1596, 1528, 1512, 1503, 1459, 1454, 1413, 1373, 1337, 1317, 1235, 1215, 1171, 1160, 1085, 1047, 1035, 1007, 981, 926, 912, 894, 830, 821, 653, 531 cm^{-1}. Raman (1000-800 cm^{-1}): 950, 924, 916, 904 cm^{-1}. TG-DTA: 473~563 K, 8.3% (exothermic); 563~733 K, 7.5% (exothermic). The crystal phase of EDATM was orthorhombic (space group C2) phase with a = 10.925, b = 13.928, c = 7.555 Å, $\alpha = \beta = \gamma = 90°$, Vc = 1151.2 $Å^3$ and Z = 8. The structure model was refined to R_{wp} = 7.30% and R_p = 14.56% for 214 reflection peaks.

$(NH_3CH_2CH(NH_3)CH_3)Mo_3O_{10}\cdot H_2O$ (1,2–PDATM): Anal. Calcd for $(NH_3CH_2CH(NH_3)CH_3)Mo_3O_{10}\cdot 1H_2O$: C, 6.6; H, 2.6; N, 5.2. Found: C, 6.9; H, 2.4; N, 5.4. IR (1700-500 cm^{-1}): 1605(s), 1580(s), 1508(s), 1460, 1407, 1395, 1368, 1336, 1317, 1218, 1163, 1080, 1052, 1023, 937(s), 884(s), 861, 765, 718(s), 664(s), 608(s) cm^{-1}. Raman (1000-800 cm^{-1}): 952, 924, 904, 894, 862, 831 cm^{-1}. TG-DTA: 403~573 K, -8.6% (exothermic); 537~723 K, -8.5% (exothermic).

$(NH_3CH_2CH_2CH_2NH_3)Mo_3O_{10}\cdot H_2O$ (1,3–PDATM) : Anal. Calcd for $(NH_3CH_2CH_2CH_2NH_3)Mo_3O_{10}\cdot 1H_2O$: C, 6.6; H, 2.6; N, 5.2. Found: C, 6.7; H, 2.8; N, 5.2. IR (1700-500 cm^{-1}): 1625(s), 1513(s), 1471(s), 1409, 1202(s), 1121(s), 1049, 937(s), 926(s), 910(s), 886(s), 862, 750, 653(s), 529(s) cm^{-1}. Raman (1000-800 cm^{-1}): 952, 911, 892, 883, 876 cm^{-1}. TG-DTA: 423~553 K, -7.5% (exothermic); 553~803 K, -9.6% (exothermic).

Synthesis of orthorhombic MoVO complex oxide. MoVO complex oxides were synthesized by using the alkylammonium isopolymolybdates and vanadyl sulfate under hydrothermal condition at 448 K for 48 h. The obtained samples were abbreviated as MoVO-(alkylammine). Dark gray samples were obtained after the hydrothermal synthesis, except with PAHM. Of key importance is the pH of precursor solution in synthesizing the crystalline MoVO complex oxide. In the case of AHM, orthorhombic MoVO can be synthesized at the range of pH value from 2.7 to 3.4 [47]. The pH=4.1 in the PAHM solution was high probably due to the occluded amine and thus prevented the formation of MoVO oxide. The pH value of the other precursor solution after mixing with vanadyl sulfate was 3.2 (MoVO-MA), 2.5 (MoVO-EA), 2.7 (MoVO-DMA), 2.6 (MoVO-TMA), 3.0 (MoVO-EDA), 2.5 (MoVO-1, 2-PDA), and 2.8 (MoVO-1, 3-PDA). Except for MoVO- PA, the pH values were within the range for forming the orthorhombic structure.

Fig. 3 shows XRD patterns of the synthesized MoVO complex oxides. The characterization results by XRD, ICP and XPS are also listed in Table 2 and 3. All of the obtained samples possessed diffraction peaks at 2θ= 22° and 45°. These two peaks can be attributed to (001) and (002) planes, respectively, indicating that the materials have a layer-type crystal structure. Moreover, the diffraction patterns of MoVO–A, MoVO–MA and MoVO–DMA catalysts showed the orthorhombic phase. We have previously reported the indexing of these materials in detail [18, 22]. No peaks related to any impurities were observed in these three samples. The anion unit of alkylammonium isopolymolybdate was $Mo_7O_{24}^{6-}$ for AHM and MAHM, and $Mo_3O_{10}^{2-}$ for DMATM. $Mo_7O_{24}^{6-}$ and $Mo_3O_{10}^{2-}$ anion species in precursor solution, therefore, seems to have less effects on the formation of the orthorhombic MoVO. The MoVO–A, MoVO–MA and MoVO–DMA catalysts were fibrous rod particles, which is also unaffected by the alkylammonium cations, as shown in Fig. 4.

On the other hand, MoVO–TMA, MoVO–EA, MoVO–EDA and MoVO–1, 2–PDA samples had diffraction patterns different from MoVO–A. The broad peaks around 2θ = 8°, 27° were observed in addition to 22° and 45°, indicating that these materials were crystallized in the c-direction only but disordered in the other directions. In a similar fashion to those reported previously [17, 48], here in this paper this material is designated as amorphous MoVO. The MoVO–1,3–PDA sample contained $(NH_4)_{0.38}V_2O_5$ and $(NH_4)_2Mo_3O_{10}$ phases.

Table. 2 Crystalline phase and the yield of various MoVO

Catalyst	Crystalline phase	Yield[1] [%]
MoVO-A	Orthorhombic	30.0 (11.6)
MoVO-MA	Orthorhombic	40.0 (11.6)
MoVO-DMA	Orthorhombic	58.2 (17.3)
MoVO-TMA	Amorphous[2]	44.4 (9.3)
MoVO-EA	Amorphous[2]	47.8 (9.7)
MoVO-EDA	Amorphous[2]	79.6 (13.3)
MoVO-1,2-PDA	Amorphous[2]	87.9 (10.0)
MoVO-1,3-PDA	Amorphous[2], $(NH_4)_{0.38}V_2O_5$ and $(NH_4)_2Mo_3O_{10}$ phases	90.0 (8.3)

1 Yield after purification was noted in brackets.

2 Amorphous Mo_3VO_x material well-crystallized in c-direction but disordered in the other direction.

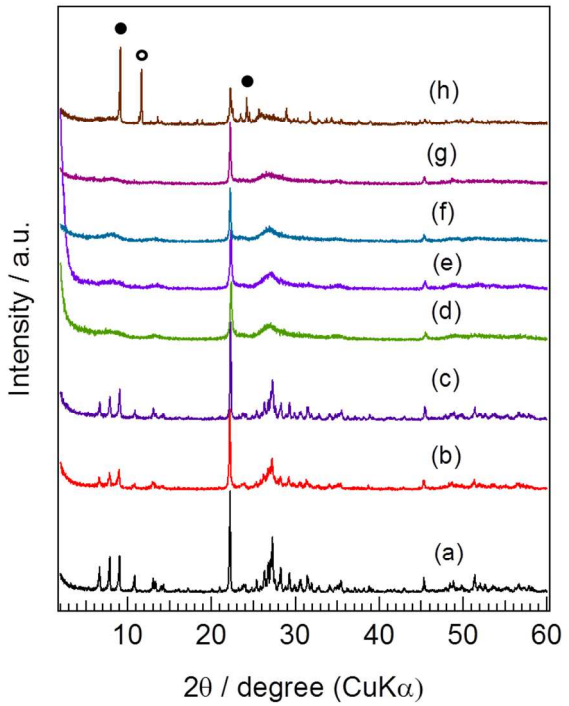

Fig. 3 XRD patterns of (a) MoVO-A; (b) MoVO-MA; (c) MoVO-DMA; (d) MoVO-TMA; (e) MoVO-EA; (f) MoVO-EDA; (g) MoVO-1,2-PDA; (h) MoVO-1,3-PDA. ($(NH_4)_{0.38}V_2O_5$(●) and $(NH_4)_2Mo_3O_{10}$ (○)phases has been marked with the pattern (h).

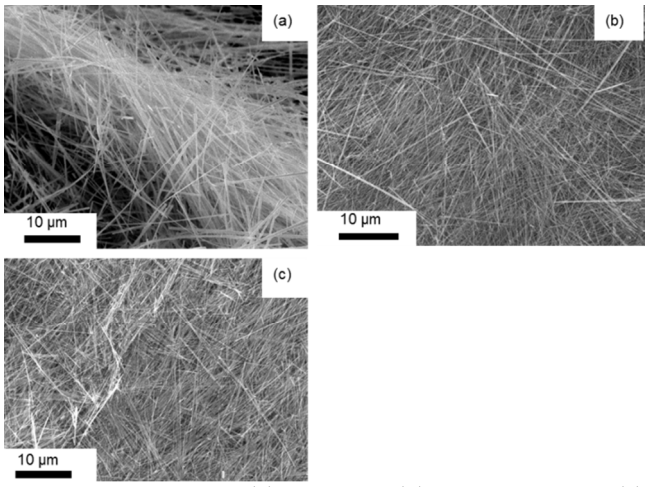

Fig. 4 SEM images of (a) MoVO-A; (b) MoVO-MA; and (c) MoVO-DMA.

It is reported that the only difference between orthorhombic and amorphous MoVO complex oxide was the elemental arrangement in the *a*-*b* plane of crystal structure. In fact, all the obtained samples showed fibrous rod morphology by SEM (not shown). The yields of MoVO-TMA, -EA, -EDA, -1, 2-PDA and -1, 3-PDA before purification were higher than that of MoVO-A. However, these large alkylammonium cations inhibit the formation for periodic arrays of the pentagonal $\{Mo_6O_{21}\}$ unit and MO_6 (M = Mo, V) octahedral unit, such that they accelerate the random condensation of units for amorphous MoVO.

The obtained orthorhombic Mo_3VO_x using the alkylammonium isomolybdates were characterized by Mo/V ratio in bulk and on surface by ICP and XPS, and by CHN elemental analysis. The elemental composition of MoVO-A has been determined to be $Mo_{28.6}V_{11.4}O_{112}(NH_4)_{3.7}\cdot 10.0H_2O$ in our previous work [20]. In the present study, the compositions of MoVO-MA and MoVO-DMA were determined to be $Mo_{32.3}V_{7.7}O_{112}(CH_3NH_3)_{4.0}\cdot 9.7H_2O$ and $Mo_{30.2}V_{9.8}O_{112}((CH_3)_2NH_2)_{2.5}\cdot 8.5H_2O$, respectively, where the corresponding alkylammonium cations were occluded in the orthorhombic structure of MoVO. The Mo/V atomic ratios both in MoVO-MA and MoVO-DMA were appreciably higher than that in MoVO-A. The reason for this change is unclear at the present stage. On the other hand, the orthorhombic structure was practically unaffected at all by the presence of the alkylammonium cations in the structure. The lattice parameters changed only slightly when the alkylammonium cations were incorporated; the lattice parameters (Å) for MoVO-MA were *a*= 21.15 *b*= 26.48 *c*= 4.00, for MoVO-DMA were *a*= 21.06 *b*= 26.49 *c*= 4.00, and for MoVO-A were *a*= 21.05 *b*= 26.47 *c*= 4.00, respectively.

Ammonium cation plays an important role in the formation of the orthorhombic Mo_3VO_x mixed-metal oxide from AHM and vanadyl sulfate under hydrothermal conditions. The $\{Mo_6O_{21}\}$ and $\{MO_6\}$(M=Mo or V) units are first formed and then start condensation to form the heptagonal channels with occluding NH_4^+ cation. NH_4^+ cation is, therefore,

Table. 3 List of the catalyst abbreviation and elemental composition of synthesized orthorhombic MoVO using various isopolymolybdate precursors

Catalyst	Mo precursor	The ratio of Mo/V			Composition of catalyst[b]	Lattice parameter
		Preparative[a]	ICP	XPS		
MoVO-A	AHM	1 / 0.25	1 / 0.38	1 / 0.24	$Mo_{28.6}V_{11.4}O_{112}(NH_4)_{3.7} \cdot 10.0H_2O$	a= 21.05 b= 26.47 c= 3.996
MoVO-MA	MAHM	1 / 0.25	1 / 0.24	1 / 0.18	$Mo_{32.3}V_{7.7}O_{112}(CH_3NH_3)_{4.0} \cdot 9.7H_2O$	a= 21.15 b= 26.48 c= 3.997
MoVO-DMA	DMATM	1 / 0.25	1 / 0.32	1 / 0.21	$Mo_{30.2}V_{9.8}O_{112}((CH_3)_2NH_2)_{2.5} \cdot 8.5H_2O$	a= 21.06 b= 26.49 c= 3.995

[a] Preparative composition of elements in the slurry, [b] Calculated by CHN elemental analysis and ICP.

considered not only to neutralize the charge of metal oxide but also to play a role of promoting the structure formation and stabilization of the orthorhombic phase. Fig. 5 shows the image of orthorhombic MoVO incorporated with alkylammonium cations. The diameter of the micropores attributed to heptagonal channel is estimated to be 4.0 Å [22]. The molecular size of methylammonium cation is about 3.8 Å in diameter of horizontal configuration and that of dimethylammonium cation is about 3.1 Å in diameter of the smallest configuration. Therefore, methylammonium and dimethylammonium cations could be incorporated into the heptagonal channel without collapsing the whole crystal structure and even work as a stabilizer of the crystalline orthorhombic structure. The number of heptagonal channels in the unit cell of the orthorhombic structure is 4.

Concomitantly, the number of methylammonium cation was determined to be 4.0 and that of ammonium cation was 3.7 in the unit cell. Obviously, these cations fully occupied the heptagonal channel. The steric hindrance is considered to be excluded the possibility of the vertical array of methylammonium cation, thus, methylammonium cation might be arrayed horizontally. On the other hand, dimethylammonium cations can locate only in a longitudinal direction in the heptagonal channel. Large cation cannot exist periodically because of the unit cell length in the *c*- direction (4.00 Å). In fact, the number of dimethylammonium cations in the unit cell of MoVO-DMA was 2.5, which suggests that 62.5% of heptagonal channel was occupied and the other may be occupied by H^+.

The amorphous MoVO were formed when TMATM, EATM, EDATM and 1, 2–PDATM used as Mo precursors. The molecular size of trimethylammonium cation, ethylendiammonium cation, and 1,2-propyldiammonium cation are undoubtedly much larger than that of heptagonal channel, indicating that these cations are unable to accommodate in the heptagonal channel such as smaller alkylammonium cations. However, the MoVO were synthesized from these alkylammonium isopolymolybdates in relatively high yield as listed in Table 2. Apparently, these cations promoted the condensation of $\{Mo_6O_{21}\}$ and $\{MO_6\}$(M=Mo or V) units although the promotion was to the direction of the formation of amorphous-type phase. It is interesting to note that dimethylammonium cation induced to form the orthorhombic MoVO while amorphous MoVO was formed when ethylammonium cation was introduced, even though the cation size of ethylammonium cation is almost the same as that of dimethylammonium cations. The slight difference of cation size would be decisive factor for the formation of orthorhombic structure under hydrothermal conditions.

The existence of the alkylammonium cations in the MoVO was also proven using FT-IR spectroscopy. Fig. 6 illustrates FT-IR spectra of the synthesized MoVO samples. According to the previous IR study on MoVO materials, the absorption at 875 cm^{-1} assigned to symmetric stretching vibrations of the Mo=O cis-dioxo groups, while absorption at 799, 720 and 646 cm^{-1} are due to antisymmetric vibrations of Mo–O–Me (Me= Mo, V) bridging bond [9, 49]. Moreover, absorption bands at 915, 601 cm^{-1} relate to V=O groups and V–O–Me (Me= Mo) bonds. All these absorption bands based on the metal-oxygen bonds were observed in the present MoVO samples, revealing that the basic structure of the metal oxide framework is the same. Detailed analyses of the FT-IR spectra of alkylammonium in the orthorhombic MoVO synthesized by AHM, MAHM and DMATM were conducted in Fig. 6b.

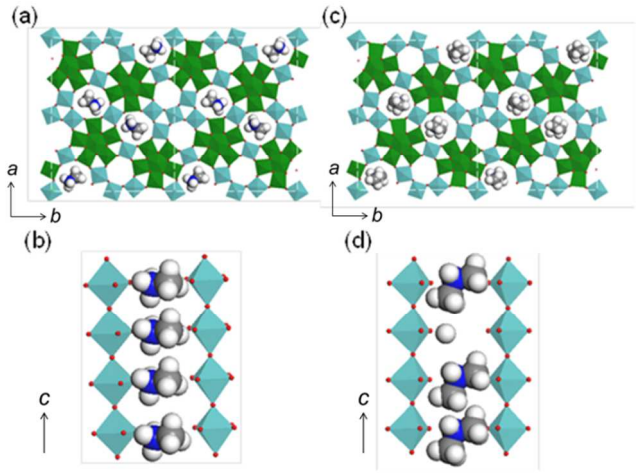

Fig. 5 Polyhedral presentations of a-b plane and the image of heptagonal channel for MoVO-MA (a, b) and MoVO-DMA (c, d). (green: pentagonal $\{Mo_6O_{21}\}$ unit, light blue: Mo or V octahedral, red: oxygen, blue: nitrogen, gray: carbon and white: hydrogen)

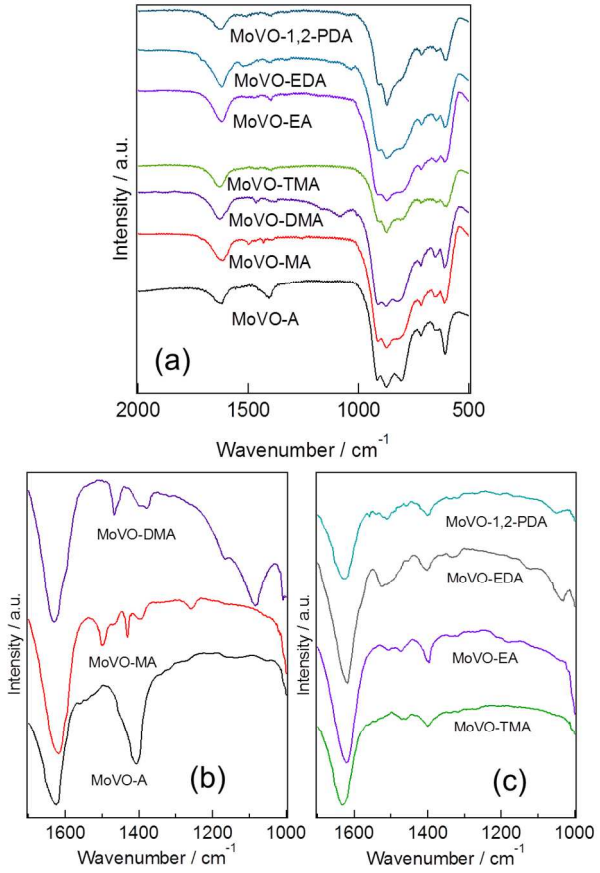

Fig. 6 IR spectra of (a) synthesized MoVO catalyst, (b) enlarged spectra of orthorhombicMoVO-A, MoVO-MA and MoVO-DMA, (c) enlarged spectra of MoVO-TMA, MoVO-EA, MoVO-EDA, MoVO-1,2-PDA, MoVO-1,3-PDA.

In the IR spectra of MoVO-A, adsorption at 1401 cm^{-1} assigned to an asymmetric deformation vibration of the ammonium cation. In MoVO-MA, the bands at 1451 and 1466 cm^{-1} assigned to asymmetric deformation vibration of the CH_3 vibration and C–H stretching and the band at 1499 cm^{-1} assigned to deformation vibration of NH_3^+ were observed [50, 51]. In MoVO-DMA, the band at 1080 cm^{-1} assigned to the stretching vibration of C-N-C bond was observed in addition of CH_3 vibration adsorption. These results are clear evidences that can support the existence of alkylammonium species in the structure of MoVO.

The IR spectra of MoVO-TMA, MoVO-EA, MoVO-EDA and MoVO-1,2-PDA are shown in Fig. 6c. There showed the adsorption bands on its alkylamine or alkylammonium cation [52, 53], but were of low intensity in the MoVO samples synthesized with lager alkylammonium cations. The spectra of these amorphous MoVO samples shows the adsorption at 1396 cm^{-1} assigned to an asymmetric deformation vibration of the ammonium ions, suggesting that the alkylammonium cations were decomposed to ammonium cations.

Microporosity of synthesized orthorhombic MoVO complex oxide. We have previously reported that the orthorhombic MoVO synthesized by AHM shows N_2 absorption of type I which is typical for microporous materials [23]. Ammonium cations can be removed from the heptagonal channel by heat treatment at 673K in air without collapse of the structure and microporosity derived from the empty heptagonal channel appears[22]. Microporosity in MoVO-MA and MoVO-DMA should be also expected similar to MoVO-A if the alkylammonium cations can be removed without collapsing the crystal structure. Therefore, N_2 adsorption isotherms were measured for MoVO-MA and MoVO-DMA before and after calcination. The MoVO-MA and MoVO-DMA samples were first calcined at 673K in air for 2 h and then further pretreated at 673K for 2 h under vacuum just before N_2 adsorption measurement. As for the uncalcined samples, the heat-treatment at 423K for 2 h under the vacuum condition was only conducted. As ascertained by the XRD pattern, the crystalline structure of the orthorhombic phase was kept unchanged after the heat treatment except for a small change in the unit-cell parameters (not shown). Samples were ground well by an agate mortar and N_2 adsorption isotherms were measured at 77 K. The results are shown in Fig. 7. Clear adsorption of N_2 at low pressure ($P/P_o \approx 10^{-7}$) was observed in both the calcined MoVO-MA and MoVO-DMA samples, while such adsorption was not observed in both the uncalcined samples. Adsorption at low pressure below 10^{-5} P/P_o is the indication of microporosity, so that it is evident that the calcined MoVO-MA and MoVO-DMA samples are a microporous material. The results at the same time support that methylammonium and dimethylammonium cations were incorporated into heptagonal channel and these cations were removed by the calcination in air, leaving empty heptagonal channels.

External surface area was calculated by the *t*-plot method. The external surface area of MoVO-MA and MoVO-DMA were 18.6 and 15.9 $m^2\ g^{-1}$, which were larger than

that of MoVO-A (7.3 $m^2 g^{-1}$). According to the results of SEM image (Fig. 4), the shape of the particle is responsible for the increase of external surface area. Fig. S3 illustrates the distribution of particle diameters obtained from analysis of SEM images. The average diameter was 0.22 μm (MoVO-MA) and 0.15 μm (MoVO-DMA), which were smaller than that of MoVO-A (0.42 μm).

This means that longer fibrous MoVO were synthesized by using methylammonium or dimethylammonium cations than by ammonium cation.

Fig. 8 shows the TPD profile of (a) MoVO-MA and (b) MoVO-DMA samples. The rate of temperature increase was 10 K min^{-1} for the desorption of species formed by the decomposition of alkylammonium cation under the TPD in flowing He. Several desorption of NH_3 (m/z=16), CO and N_2 (m/z=28), and CO_2 (m/z=44) were observed at 603K in both MoVO-MA and MoVO-DMA samples. The high temperature desorption of these species clearly proves that alkylammonium cations existed in the heptagonal channel are decomposed.

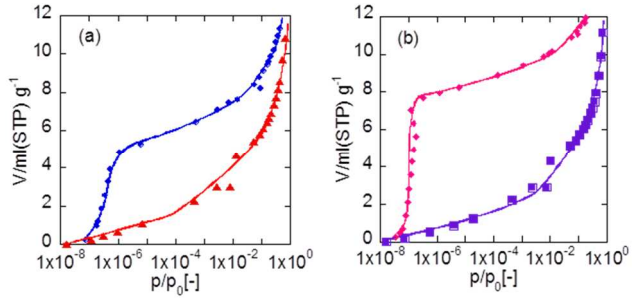

Fig.7 Adsorption isotherms of (a) MoVO-MA and (b) MoVO-DMA. ▲, ■: samples were dried with air at 373K, ●, ♦: samples were heat-treated under air flow at 673 K.

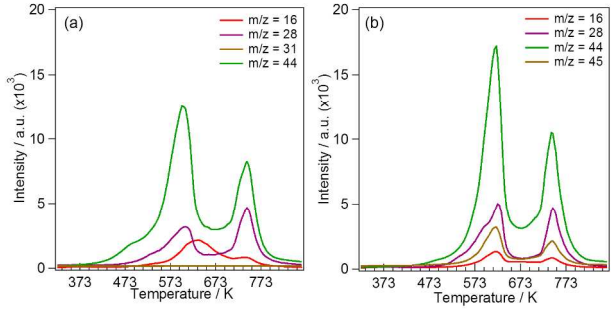

Fig. 8 TPD spectra of synthesized MoVO-MA (a) and MoVO-DMA (b). Samples were outgassed at 423 K under vacuum for 2h.

Catalytic activity of synthesized MoVO samples. The catalytic activity of the synthesized orthorhombic MoVO was tested in the oxidative dehydrogenation of ethane (Table 4). After the reaction, XRD patterns confirmed that the structures remained unchanged. External surface area and pore volume of the catalysts after the reaction were calculated by the *t*-plot method and are listed in Table 4. The pore volume of MoVO-DMA was larger than that of MoVO-A and MoVO-MA, potentially due to the different configuration of the counter cations in the heptagonal channel. MoVO-A showed high catalytic activity for the reaction as reported previously [19, 48]. Similarly, MoVO-MA and MoVO-DMA showed the conversion of 24% and 28%, which is a little higher compared to that of MoVO-A.

Table. 4 The results of nitrogen adsorption and selective oxidation of ethane over the synthesized orthorhombic MoVO catalysts at 300°C[a]

catalyst	Aext[b] [$m^2 g^{-1}$]	Pvol[c] [$cm^3 g^{-1}$]	Temp. [°C]	C_2H_6 conv. [%]	Sel. [%] C_2H_4	Sel. [%] CO_x	Sel. [%] AcOH[d]
MoVO-A	7.2	0.0130	300.1	20.9	83.4	12.5	3.0
MoVO-MA	16.7	0.0137	298.8	23.7	86.0	9.1	3.6
MoVO-DMA	15.0	0.0161	298.8	28.3	87.2	8.6	3.8

a Reaction conditions: 0.5 g catalyst, flow rate 50 ml min-1, composition $C_2H_6/O_2/N_2$ = 1: 1: 8, b Aext: External surface area calculated by t-plot, c Pvol : pore volume calculated by t-plot, d AcOH : Acetic acid

The selectivity to ethylene was also slightly higher in the MoVO-MA catalyst and the MoVO-DMA catalysts. The active site of ethane oxidation has been suggested not to relate to the lateral face of the rod particle, rather to the heptagonal channel of the *a*-*b* plane by comparison of the catalytic activity using several crystalline structures [48]. The present work also supports that the ethane oxidation takes place in the heptagonal channel, since the three samples with the same crystalline structure showed comparable catalytic activity although different external surface areas.

CONCLUSIONS

Various alkylammonium isopolymolybdates were synthesized by the evaporation or by precipitation methods and pure materials comprised of methylammonium heptamolybdate, dimethylammonium trimolybdate, ethylammnium trimolybdate and ethylenediammonium trimolybdate were obtained. The orthorhombic MoVO materials incorporating methylammonium and dimethylammonium cations in their heptagonal channel were synthesized for the first time by using the corresponding alkylammonium isopolymolybdate. The morpholgy of the crystalline particles were fibrous and their diameters were much small compared with MoVO-A. These alkylammonium cations could act as a stabilizer for the orthorhombic structure under hydrothermal conditions. The incorporated cations were removed from the synthesized Mo-

VO complex oxide by the calcination. The pore volume of MoVO-DMA was larger than that of MoVO-A and MoVO-MA, suggesting that dimethylammonium cation assists well-arrangement of the heptagonal channel. The formation of the micropore resulted in the catalytic activity for ethane selective oxidation.

ASSOCIATED CONTENT

Supporting Information.

Preparation conditions of alkylammonium isopolymolybdates, XRD data of alkylammonium isopolymolybdate, the refinements results by Pawley method, distribution of the diameter of MoVO particle, TPD spectra of calcined MoVO. This material is available free of charge via the Internet at http://pubs.acs.org.

AUTHOR INFORMATION

Corresponding Author

*E-mail: murayama@cat.hokudai.ac.jp (T. Murayama); ueda@cat.hokudai.ac.jp (W. Ueda)

Funding

This work has been supported by JSPS KAKENHI Grant Number 2324-6135.

REFERENCES

[1] T. Ushikubo, H. Nakamura, Y. Koyasu, S. Wajiki, *US Patent*. **1995**, 5,380,933.

[2] M. Lin, T. Desai, F. Kaiser, P. Klugherz, *Catal. Today*. **2000**, *61*, 223–229.

[3] F. Ivars, B. Solsona, E. Rodriguez-Castellón, J.M. López Nieto, *J. Catal*. **2000**, *262*, 35–43.

[4] B. Deniau, J.M.M. Millet, S. Loridant, N. Christin, J.L. Dubois, *J. Catal*. **2008**, *260*, 30–36.

[5] X. Tu, N. Furuta, Y. Sumida, M. Takahashi, H. Niiduma, *Catal. Today*. **2006**, *117*, 259–264.

[6] R. Feng, X.J. Yang, W.-J. Ji, H.-Y. Zhu, X.-D. Gu, Y. Chen, S. Han, H. Hibst, *J. Mol. Catal. A: Chem*. **2007**, *267*, 245–254.

[7] T. Ushikubo, K. Oshima, A. Kayou, M. Hatano, *Stud. Surf. Sci. Catal*. **1997**, *112*, 473–480.

[8] M. Aouine, J.L. Dubois, J.M.M. Millet, *Chem. Commun*. **2001**, *13*, 1180–1181.

[9] (a) P. Botella, B. Solsona, A. Martinez-Arias, J.M. López Nieto, *Catal. Lett*. **2001**, *74*, 149–154; (b) P. Botella, J.M. López Nieto, B. Solsona, A. Mifsud, F. Marquez, *J. Catal*. **2002**, *209*, 445–455.

[10] J.M. Oliver, J.M. López Nieto, P. Botella, *Catal. Today*. **2004**, *96*, 241–249.

[11] (a) R.K. Grasselli, J.D. Burrington, D.J. Buttery, P. Desanto Jr., C.G. Lugmair Jr., A.F. Volpe Jr., T. Weingand, *Top. Catal*. **2003**, *23*, 5–22; (b) P. DeSanto, D.J. Buttreya, R.K. Grasselli, C.G. Lugmair, A.F. Volpe, B.H. Tobyc, T. Vogt, *Top. Catal*. **2003**, *23*, 23–38.

[12] M. Baca, A. Pigamo, J.L. Dubois, J.M.M. Millet, *Top. Catal*. **2003**, *23*, 39–46.

[13] E. García-González, J.M. López Nieto, P. Botella, J.M. González-Calbet, *Chem. Mater*. **2002**, *14*, 4416–4421.

[14] J.M.M. Millet, H. Roussel, A. Pigamo, J.L. Dubois, J.C. Jumas, *Appl. Catal. A: Gen*. **2002**, *232*, 77–92.

[15] M. Baca, M. Aouine, J.L. Dubois, J.M.M. Millet, *J. Catal*. **2005**, *233*, 234– 241.

[16] N.R. Shiju, V.V. Guliants, *ChemPhysChem*. **2007**, *8*, 1615.

[17] W. Ueda, K. Oshihara, D. Vitry, T. Himeno, Y. Kayashima, *Catalysis surveys from Japan*. **2002**, *6*, Nos. 1/2, 33-44.

[18] W. Ueda, D. Vitry, T. Kato, N. Watanabe, Y. Endo. *Res. Chem. Intermed.* **2006**, *32*, No. 3–4, 217–233.

[19] T. Katou, D. Vitry, W. Ueda. *Catal. Today*, **2004**, *91-92*, 237-240.

[20] N. Watanabe, W. Ueda. *Ind. Eng. Chem. Res*. **2006**, *45*, 607-614.

[21] M. Sadakane, K. Kodato, T. Kuranishi, Y. Nodasaka, K. Sugawara, N. Sakaguchi, T. Nagai, Y. Matsui, W. Ueda, *Angew. Chem. Int. Ed*. **2008**, *47*, 2493 -2496.

[22] M. Sadakane, K. Yamagata, K. Kodato, K. Endo, K. Toriumi, Y. Ozawa, T. Ozeki, T. Nagai, Y. Matsui, N. Sakaguchi, W. D. Pyrz, D. J. Buttrey, D. A. Blom, T. Vogt, W. Ueda, *Angew. Chem. Int. Ed*. **2009**, *48*, 3782 –3786.

[23] M. Sadakane, S. Ohmura, K. Kodato, T. Fujisawa, K. Kato, K. Shimidzu, T. Murayama, W. Ueda, *Chem. Commun*. **2011**, *47*, 10812–10814.

[24] W. D. Pyrz, D. A. Blom, M. Sadakane, K. Kodato, W. Ueda, T. Vogt, D. J. Buttrey, *Chem. Mater*. **2010**, *22*, 2033-2040.

[25] W. D. Pyrz, D. A. Blom, M. Sadakanec, K. Kodato, W. Ueda, T. Vogt, D. J. Buttrey, *PNAS*. **2010**, *107*, 6153.

[26] A. Müller, P. Kögerler, A. W. M. Dress, Coord. *Chem. Rev*. **2001**, *222*, 193.

[27] A. Müller, E. Krichemeyer, H. Bögge, M. Schmidtmann, F. Peters, *Angew. Chem. Int. Ed*. **1998**, *37*, 3360-3363.

[28] A. Müller, S.-Q.-N. Shah, H. Bögge, M. Schmidtmann, *Nature*, **1999**, *397*, 48-50.

[29] A. Müller, S. Polarz, S. K. Das, E. Krichemeyer, H. Bögge, M.Schmidtmann, B. Hauptfleisch, *Angew. Chem. Int. Ed*. **1999**, *38*, 3241-3245.

[30] M. Sadakane, N. Watanabe, T. Katou, Y. Nodasaka, W. Ueda, *Angew. Chem. Int. Ed*. **2007**, *46*, 1493 –1496.

[31] N. Yamazoe, L. Kihlborg, *Acta Cryst*. **1975**, B31, 1666.

[32] P. J. Hagrman, R. C. Finn, J. Zubieta, *Solid State Sci*. **2001**, *3*, 745–774.

[33] Y. Xu, M. Ogura, T. Okubo, *Micropor. Mesopor. Mater*. **2004**, *70*, 1-6.

[34] F. O. M. Gaslain, K. E. White, A. R. Cowley, A. M. Chippindale, *Micropor. Mesopor. Mater*. **2008**, *112*, 368-376.

[35] J.V. Smith, *Chem. Rev*. **1988**, *88*, 149.

[36] C.T. Kresge, M.E. Leonowicz, W.J. Roth, J.C. Vartuli, J.S. Beck, *Nature*, **1992**, *359*, 710.

[37] O. Trofymluk, A. A. Levchenko, A. Navrotsky, *Micropor. Mesopor. Mater*. **2012,** *149*, 119-125.

[38] S. Mann, *Nature*, **1993**, *65*, 499.

[39] R.C. Haushalter, L.A. Mundi, *Chem. Mater*. **1992**, *4*, 31.

[40] M.I. Khan, L.M. Meyer, R.C. Haushalter, A.L. Schweitzer, J. Zubieta, J.L. Dye, *Chem. Mater*. **1996**, *8*, 43.

[41] S. Himeno, H. Niiya, T. Ueda, *Bull. Chem. Soc. Jpn*. **1997**, *70*, 631-637.

[42] T. Zeegers-Huyskens, G. Bator, *Vib. Spectrosc*. **1996**, *13*, 41-49.

[43] H. Toraya, F. Marumo, T. Yamase, *Acta Cryst*. **1984**, *B40*, 145-150.

[44] N. Guillou, G. Ferey, *J. Solid State Chem*. **1997**, *132*, 224-227.

[45] C. Ding, B-Z. Lin, G-H. Han, L. Bai, *Acta Cryst*. **2007**, *C63*, 256-258.

[46] W. Bensch, P. Hug, R. Emmenegger, A. Reller, H. R. Oswald, *Mater. Res. Bull*. **1987**, 22, 447-454

[47] M. Sadakane, K. Endo, K. Kodato, S. Ishikawa, T. Murayama, W. Ueda, *Eur. J. Inorg. Chem. in press*.

[48] T. Konya, T. Katou, T. Murayama, S. Ishikawa, M. Sadakane, D. Buttrey, W. Ueda, *Catal. Sci. Technol*. **2013**, *3*, 380-387.

[49] P. Botella, P. Concepcion, J. M. Lopez Nieto, B. Solsona, *Catal. Lett*. **2003**, *89*, 3–4, 249-253.
[50] I. A. Oxton, O. Knop, J. L. Duncan, *J. Mol. Struct*. **1977**, *38*, 25-32.
[51] D. J. DeFrees, A.D. McLean, *J. Chem. Phys*. **1985**, *82*, 333-341.
[52] I. A. Oxton, O. Knop, *J. Mol. Struct*. **1978**, *43*, 17-28.
[53] I. A. Oxton, *J. Mol. Struct*. **1979**, *54*, 11-18.

Authors are required to submit a graphic entry for the Table of Contents (TOC) that, in conjunction with the manuscript title, should give the reader a representative idea of one of the following: A key structure, reaction, equation, concept, or theorem, etc., that is discussed in the manuscript. Consult the journal's Instructions for Authors for TOC graphic specifications.

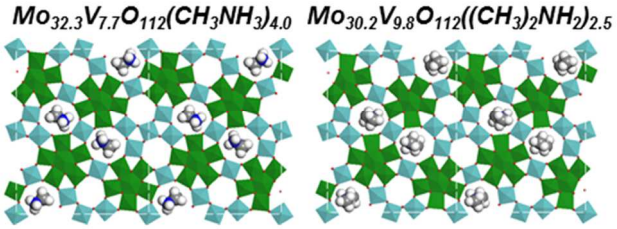

Supporting Information

Preparation of alkylammonium isopolymolybdate by evaporation.

Alkylammonium isopolymolybdates were prepared by evaporation method. 22.594 g of MoO_3 (Kanto; 0.150 mol) was added into the mixed solutions prepared each amount of the amine solution and water, followed by the stirring for 30 min. The reason for the water addition is to reduce the viscosity of the mixed solutions. The amine solutions used this time were 40% methylamine solution, 40% dimetylamine solution, 30% trimethylamine solution, 70% ethylamine solution, 98% of propylamine, 99% of etylenediamine, 99% of 1,2-propanediamine, and 97% of 1,3-propanediamine, respectively. All of the reagents were purchased from Wako. The amounts of the amine solution and water are shown in Table S1. After MoO_3 was dissolved completely, the mixed solutions were evaporated under vacuumed condition of P/P_0= 0.03 at 343 K for 30 min. Time was measured from the time that white powder was started to precipitate. Obtained powder was dried in air at 353 K overnight. Prepared alkylammonium isopolymolybdates are abbreviated as Table S1.

Table. S1 Amount of amine solution and water for preparing alkylammonium isopolymolybdates and the name of the obtained materials

	Amount of amine [ml]	Amount of water [ml]	Abbreviation of alkylammonium isopolymolybdate
40% metylamine	33.2	0	MAHM
40% dimetylamine	50.5	0	DMATM
30% trimetylamine	88.2	0	TMATM
70% ethylamine	28.0	28.0	EATM
98% propylamine	25.2	88.2	PAHM
99% etylenediamine	20.0	40.0	EDAMM
99% 1,2-propanediamine	25.0	100.0	1,2-PDAMM
97% 1,3-propanediamine	25.0	100.0	1,3-PDADM

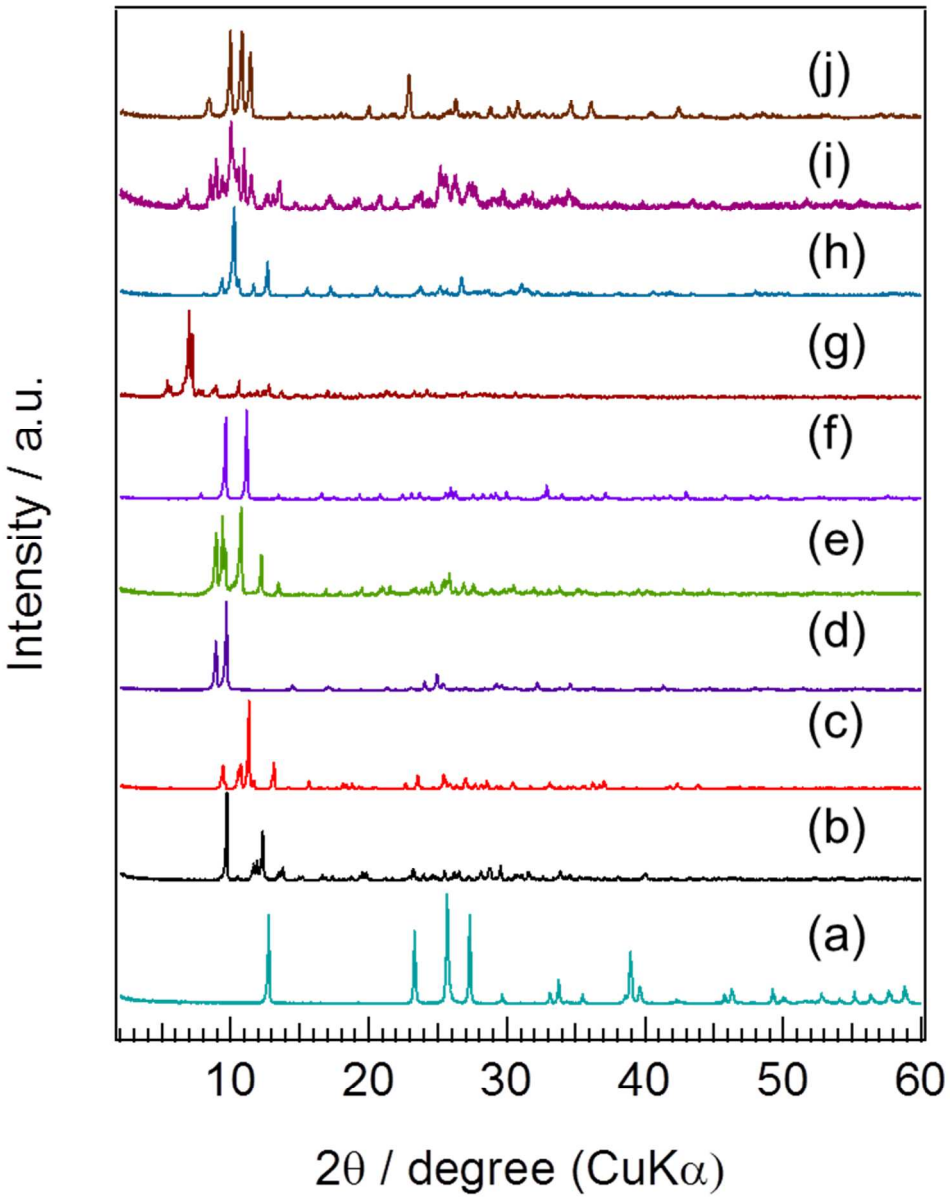

Fig. S1 Normalized XRD patterns of MoO_3 (a); AHM reagent (b), and prepared isopolymolybdate precursors: MAHM (c); DMATM (d); TMATM (e); EATM (f); PAHM (g); EDATM (h); 1,2-PDATM (i); and 1,3-PDATM (j).

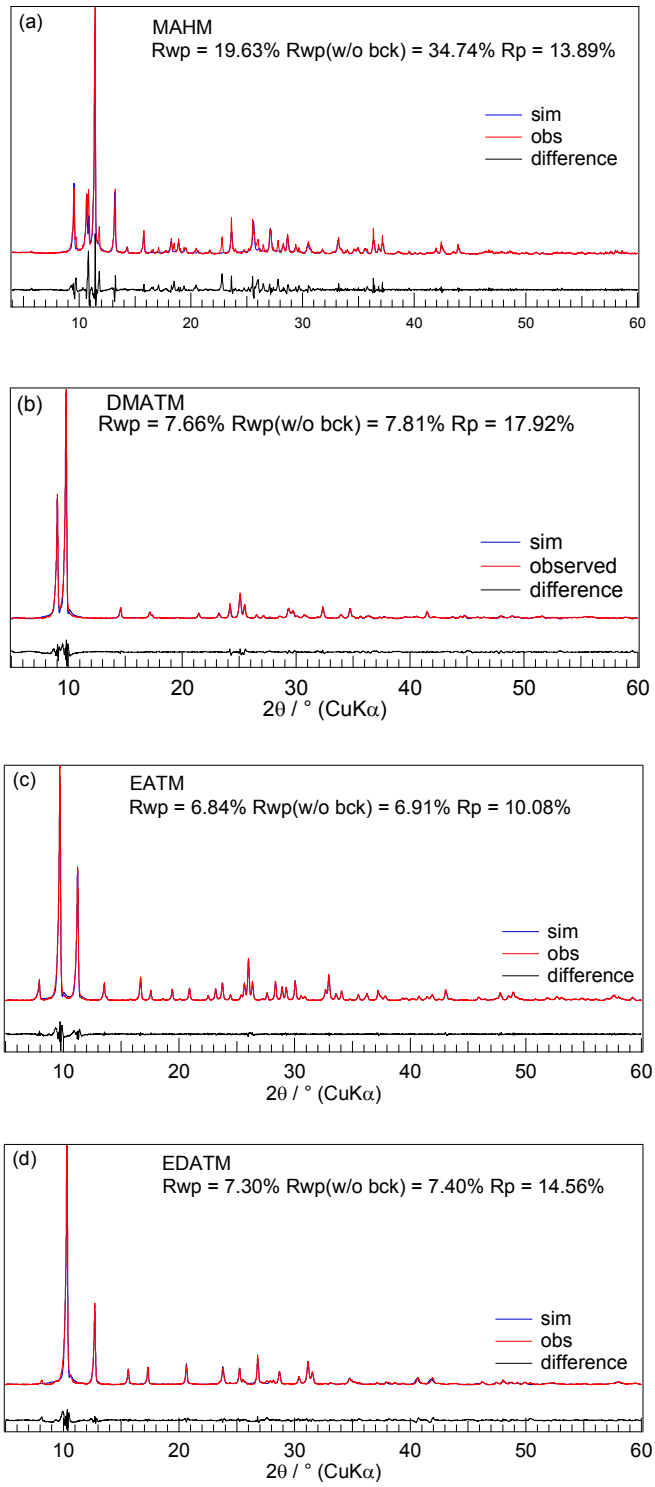

Fig. S2 The calculated results by Pawley method with the experimental results of (a)MAHM, (b)DMATM, (c)EATM and (d)EDATM. Peaks of (Int/ $Int_{max)}$> 0.10 were identified below.

MAHM : 2θ= 9.5, (110); 2θ= 10.6, (11$\bar{1}$); 2θ= 10.9, (200); 2θ= 11.4, (20$\bar{1}$); 2θ=13.2, (201); 2θ=25.6, (40$\bar{3}$); 2θ=27.1, (420)

DMATM : 2θ = 9.0, (200); 2θ= 9.8, (110); 2θ= 25.1, (420)

EATM : 2θ = 9.7, (021); 2θ= 11.2, (002); 2θ= 26.0, (202)

EDATM : 2θ = 10.3, (110); 2θ= 12.7, (020); 2θ= 26.8, (022), 2θ= 31.1, (330)

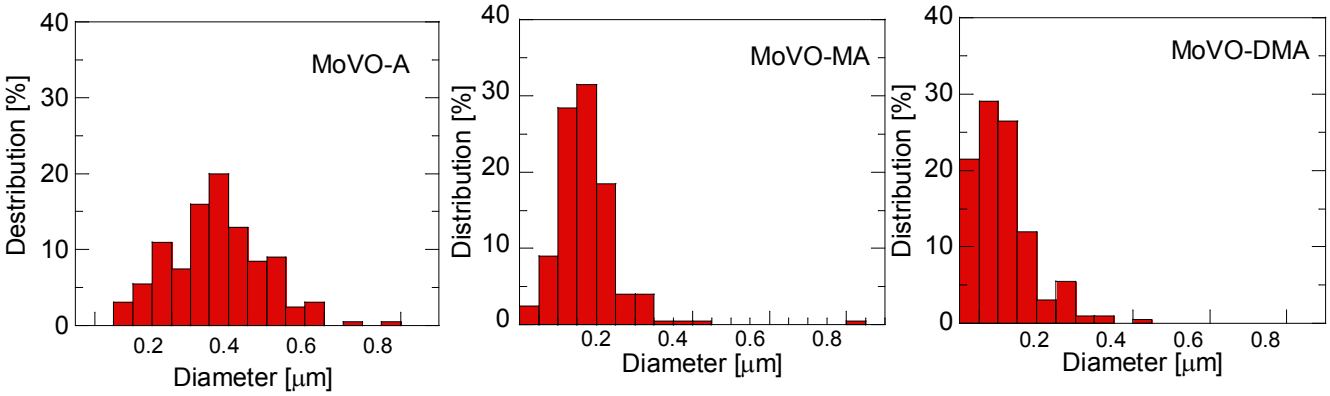

Fig. S3 Distribution of the diameter of rod particle in orthorhombic MoVO samples.

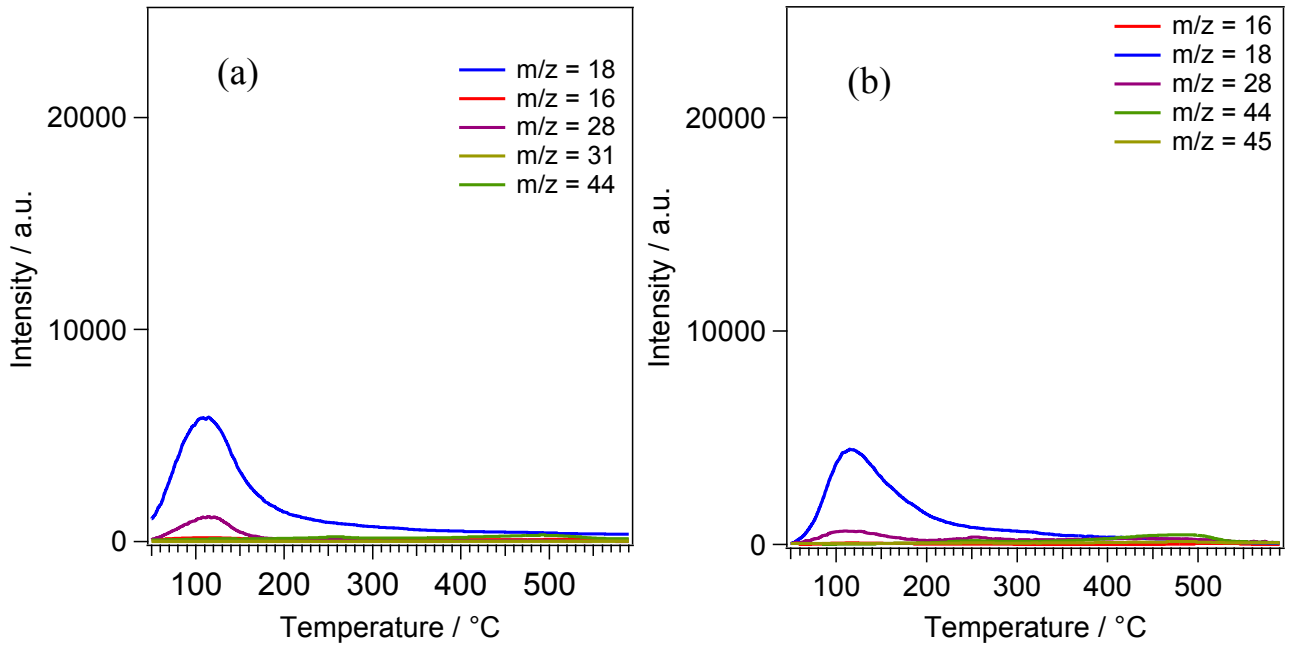

Fig. S4 TPD spectra of calcined samples. (a) MoVO-MA and (b) MoVO-DMA.